JOURNAL OF NANO- AND ELECTRONIC PHYSICS *ЖУРНАЛ НАНО- ТА ЕЛЕКТРОННОЇ ФІЗИКИ*
Vol. **7** No 4, 04084(4pp) (2015) Том **7** № 4, 04084(4cc) (2015)

The Electron Scattering on Local Potential of Crystal Defects in GaSb Whiskers

A.A. Druzhinin[1,2], I.P. Ostrovskii[1,2], Yu.N. Khoverko[1,2], I.I. Khytruk[1]

[1] *Lviv Polytechnic National University, 12, S. Bandera St., 79013, Lviv, Ukraine*
[2] *International Laboratory of High Magnetic Fields and Low Temperatures, 95, Gajowicka St., Wroclaw, Poland*

(Received 23 September 2015; published online 24 December 2015)

The concentration and mobility of electrons were examined by Hall measurements in *n*-GaSb whiskers with defect concentration of about 5×10^{17} cm^{-3}. The dependences of electron mobility and Hall factor on temperature were calculated using the short-range scattering models in the temperature interval 4.2-500 K. The electron interaction with different types of lattice defects was considered.

Keywords: Charge carrier scattering, Transport phenomena, GaSb whiskers.

PACS numbers: 42.79.Wc, 84.60.Jt

1. INTRODUCTION

Gallium antimonide based materials provide a wide range of electronic band gaps, electronic barriers along with extremely high electron mobility and therefore have been studied extensively in recent years for potential device applications in a variety of mid-infrared lasers, detectors and extremely low-power high-speed electronic devices [1-4]. But to take full advantage of the potential and functionality of antimonide-based devices, it is desirable to grow the epitaxial layers or QDs on a lattice-matched semi-insulating substrate. However, an influence of substrate substantially restricted the advantages of material free-standing nano- and microwhiskers are used to avoid shortcoming a growth of GaSb ingots.

For the transport phenomena description in this semiconductor long-range scattering models of charge carriers is mainly used. According to this models charge carrier should interacts with all the crystal (electron-phonon interaction) or with the defect potential of the impurity with the action radius equal to ~ 10-1000 a_0 (a_0 – lattice constant). But the charge carrier must interact with neighbouring crystal region in conformity with special theory of relativity. Moreover above-mentioned theories are considered in the first approximation of perturbation theory whereas the defect potential becomes the second order of the magnitude for defects with the interaction energy $U \approx 1/r^n (n = 1,2)$ on distances on distances $\sim 10a_0$. While foregoing shortcomings are absent in the proposed short-range electrons scattering models in zinc-blende and in wurtzite [5, 6] semiconductors. It is assumed that the carrier can interacts with the potential of defect which covering one cell of the crystal. The aim of the paper is to apply these models for description the electron scattering processes in gallium antimonide wiskers.

2. THEORY

According to the short-range scattering models in zinc-blende structure semiconductor the carrier transition probability from state k to state k′ which occure during the scattering on the polar optical (Po), nonpolar optical (Npo), piezooptic (Pop) and piezoacoustic (Pac), acoustic (Ac) phonons, static strain (Ss) potential, ion-ized (Ii) and neutral (Neut) impurities looks like [5, 6]:

$$W_{PO}(\mathbf{k},\mathbf{k}') = \frac{64\,\pi^7 \gamma_{PO}^{10}\, e^4}{225\,\varepsilon_0^2 a_0{}^4 G}\ \frac{M_{Ga}+M_{Sb}}{M_{Ga}\,M_{Sb}}\left\{\frac{1}{\omega_{LO}} N_{LO}\delta(\varepsilon'-\varepsilon-\hbar\omega_{LO}) + \right.$$
$$\left. + (N_{LO}+1)\delta(\varepsilon'-\varepsilon+\hbar\omega_{LO})\right] + \frac{2}{\omega_{TO}}\left[N_{TO}\delta(\varepsilon'-\varepsilon-\hbar\omega_{TO}) + (N_{TO}+1)\delta(\varepsilon'-\varepsilon+\hbar\omega_{TO})\right]\right\}; \quad (1)$$

$$W_{NPO}(\mathbf{k},\mathbf{k}') = \frac{\pi^3 E_{NPO}{}^2}{288 a_0{}^2 G}\ \frac{M_{Ga}+M_{Sb}}{M_{Ga}\,M_{Sb}}\left\{\frac{1}{\omega_{LO}} N_{LO}\delta(\varepsilon'-\varepsilon-\hbar\omega_{LO}) + \right.$$
$$\left. + (N_{LO}+1)\delta(\varepsilon'-\varepsilon+\hbar\omega_{LO})\right] + \frac{2}{\omega_{TO}}\left[N_{TO}\delta(\varepsilon'-\varepsilon-\hbar\omega_{TO}) + (N_{TO}+1)\delta(\varepsilon'-\varepsilon+\hbar\omega_{TO})\right]\right\}; \quad (2)$$

$$W_{POP}(\mathbf{k},\mathbf{k}') = \left(\frac{32}{75}\right)^2 \frac{\pi^9 e^2 e_{14}^2\, \gamma_{PZ}^{10}}{\varepsilon_0{}^2 G}\ \frac{M_{Ga}+M_{Sb}}{M_{\mathrm{Ga}}\,M_{Sb}}\left\{\frac{1}{\omega_{LO}} N_{LO}\delta(\varepsilon'-\varepsilon-\hbar\omega_{LO}) + \right.$$
$$\left. + (N_{LO}+1)\delta(\varepsilon'-\varepsilon+\hbar\omega_{LO})\right] + \frac{2}{\omega_{TO}}\left[N_{TO}\delta(\varepsilon'-\varepsilon-\hbar\omega_{TO}) + (N_{TO}+1)\delta(\varepsilon'-\varepsilon+\hbar\omega_{TO})\right]\right\}; \quad (3)$$

$$W_{PAC}(\mathbf{k},\mathbf{k}') = \frac{128\pi^7\, e^2\, e_{14}^2\, a_0^2\, \gamma_{PZ}^{10}\, k_B T}{225\,\varepsilon_0^2\,\hbar\,\mathrm{G}\left[M_{Ga}+M_{Sb}\right]}\left(\frac{1}{c_{LO}}+\frac{2}{c_{TO}}\right)^2 \delta(\varepsilon'-\varepsilon); \quad (4)$$

$$W_{AC}(\mathbf{k},\mathbf{k}') = \frac{\pi^3 k_B T\; E_{AC}^2}{144\,\hbar\,\mathrm{G}\left[M_{Ga}+M_{Sb}\right]}\left(\frac{1}{c_{||}}+\frac{2}{c_{\perp}}\right)^2 \delta(\varepsilon'-\varepsilon); \quad (5)$$

$$W_{II}(\mathbf{k},\mathbf{k}') = \frac{\pi\, e^4 Z_i^2\, N_{II}\, \gamma_{II}^4\, a_0^4}{2\,\varepsilon_0^2\,\hbar\, V}\delta(\varepsilon'-\varepsilon); \quad (6)$$

$$W_{NEUT}(\mathbf{k},\mathbf{k}') = \frac{20\pi^2 5 a_B \hbar^3 N_{NEUT}}{V m^{*2} k(\varepsilon)}\delta(\varepsilon'-\varepsilon); \quad (7)$$

$$W_{SS}(\mathbf{k},\mathbf{k}') = \frac{2^5 3^4 \pi^3 C^2 a_0^6 e^2\; e_{14}^2 N_{SS}}{V\varepsilon_0^2\hbar}\frac{1}{q^2}\delta(\varepsilon'-\varepsilon), \quad (8)$$

where M_{Ga}, M_{Sb} – the atom masses; G – the number of unit cells in a crystal volume; ε_0 – the vacuum permittivity; e – the elementary charge; k_B – the Boltzmann constant; η – the Planck constant; N_{LO}, N_{TO} – the number of longitudinal (LO) and transverse (TO) phonons with a frequency ω_{LO} and ω_{TO} respectively; e_{14} – the component of the piezoelectric tensor; $c_{||}$, $c_{\perp}$ – the respective sound velocities; V – the crystal volume; N_{II}, N_{NEUT}, N_{SS} – the ionized and neutral impurities, strain centers concentration respectively; Z_i – the impurity charge in electroncharge units; E_{AC}, E_{NPO} – the acoustic and optical deformation potentials respectively; m^* – effective mass of charge carrier; $k(\varepsilon)$ – wave vector of electron $\gamma_{PO}, \gamma_{PZ}, \gamma_{II}$ – the fitting parameters determining the action radius of short-range potential ($R = \gamma\, a_0$, $0 \le \gamma_{PO}, \gamma_{PZ} \le 0.86$, $0 \le \gamma_{II} \le 1$).

The choice opportunities of parameters $\gamma_{PO}, \gamma_{PZ}, \gamma_{II}$ numerical values is sharply limited by their strong power dependence.

Table 1 – Parameters of GaSb used in calculations

Material parameter	Value, temperature dependence	Refences
Atom masses, kg	$M_{Ga} = 11.5777 \times 10^{-26}$ $M_{Sb} = 20.2187 \times 10^{-26}$	[7]
Lattice constant, m	$a_0 = 6.09593 \times 10^{-10}$	[8]
Energy gap, eV	$E_g = 0.813\text{-}0.378 \times 10^{-3}\, T^2/(T + 94)$	[9]
Electron effective mass	$m_e/m_0 = 0.041$	[10]
Energy equivalent of matrix element, eV	$E_p = 27$	[11]
Ionization energy, eV	$E_{id} = 0.01$	[12]
Spin-orbit splitting, eV	$\Delta = 0.80$	[13]
Density, gm cm^{-3}	$\rho_0 = 5.613$	[14]
Dielectric constants	$\varepsilon_s = 15.69$ $\varepsilon_\infty = 14.44$	[15]
Sound velosity, m·s^{-1}	$c_\parallel = 4.24 \cdot 10^3$ $c_\perp = 2.46 \cdot 10^3$	[16]
Optical deformation potential, eV	ENPO = 32	[17]
Acoustic deformation potential, eV	EAC = 9.3	[18]
Optical phonon frequency, rad·s^{-1}	$\omega_{TO} = 6.90 \cdot 10^{13}$ $\omega_{LO} = 7.11 \cdot 10^{13}$	[19]
Piezoelectric tensor component, C·m^{-2}	$e_{14} = 0.126$	[20]

Table 2 – The dependence of Fermi energy in n-GaSb ($N_D = 5 \times 10^{17}$ cm^{-3}) on temperature

T, K	F, eV	n, cm^{-3}	N_{II}, cm^{-3}	N_{NEUT}, cm^{-3}
4.2	0.02336	8.64×10^{16}	8.64×10^{16}	4.13×10^{17}
15	0.02457	9.36×10^{16}	9.36×10^{16}	4.06×10^{17}
40	0.02866	1.20×10^{17}	1.20×10^{17}	3.79×10^{17}
77	0.03722	1.82×10^{17}	1.82×10^{17}	3.17×10^{17}
120	0.04956	2.86×10^{17}	2.86×10^{17}	2.13×10^{17}
160	0.06070	3.94×10^{17}	3.94×10^{17}	1.05×10^{17}
190	0.06624	4.54×10^{17}	4.54×10^{17}	4.55×10^{16}
250	0.06854	4.95×10^{17}	4.95×10^{17}	4.94×10^{15}
300	0.06702	4.99×10^{17}	4.99×10^{17}	7.48×10^{14}
400	0.06157	4.99×10^{17}	4.99×10^{17}	2.15×10^{13}
500	0.05413	4.99×10^{17}	4.99×10^{17}	7.47×10^{11}

Fermi energy was calculated from the electroneutrality equation given by:

$$n = N_D\left[2\exp\left(-\frac{E_F - E_d}{k_B T)}\right)\right]^{-1} \qquad (9)$$

where E_d – the ionization energy of donors (T_e), determined in [12]; N_D – the value of donors concentration; N_D^+ – ionized impurity concentration. Temperature dependence of the Fermi energy, electron concentration, neutral and ionized impurities concentrations are presented in Table 2. The conductivity tensor components was calculated using the formalism of the exact analytical solution of the kinetic Boltzmann equation [24]. Using this formalism we can obtain the additional fitting parameter $\gamma_{SS} N_{SS}$ (we put $\gamma_{SS} = 1$) for SS-scattering mode.

3. COMPARISON OF THEORY AND EXPEMENT

In paper [21] a comparison of theoretical and experimental data of dependences of mobility of electrons on temperature for GaSb whiskers grown by chemical vapour deposition method in bromide system was made. The whiskers were doped with Te impurity to concentration that corresponds to metal-insulator transition.The whisker diameters range from 20 to 40 μm.

Temperature investigations were conducted in temperature range 4,2-300 K at magnetic field up to 10 T [22, 23]. The samples were cooled down to 4,2 K in the helium cryostat. A special inset with the bifilar winding heater has been used to heat-up samples to the 300 K. The stabilized electrical current of 100 μA-1 mA which depend on the resistance of the the sample being studied has been generated by Keithley 224 current source. The Keithley 2000 and Keithley 2010 digital voltmeters with the simultaneous automatic registration via the parallel port of PC, the vizualization and saving the data arrays into files have been used to measure the voltage at the potential contacts of samples, the output of thermocouple and of the magnetic field sensor with the accuracy of up to 1×10^{-6} V. The Bitter-magnet based setup has been used to study the effect of strong magnetic fields on the samples. The

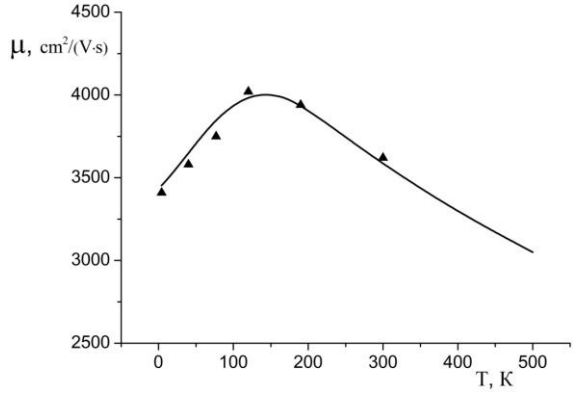

Fig. 1 – The temperature dependence of the electron mobility in n-GaSb crystal with donor concentrations $N_D = 5 \times 10^{17}$ cm^{-3}

induction of the magnet was 14 T, deflection time 1,75 T/min and 3,5 T/min at 4,2 K and higher temperature range respectively.

The theoretical dependence $\mu_n(T)$ are presented in Fig. 1. The solid line corresponds to the mobility calculated using the short-range models on the base of the exact solution of the kinetic Boltzmann equation.

It could be seen a good coincidence of the theory and experiment in the researched interval of temperatures . The obtained electron scattering parameters for different defects cases are listed in Table 3.

Table 3 – Parameters γ for different scattering modes

N_D, cm^{-3}	γ_{PO}	γ_{PZ}	γ_{II}	$\gamma_{SS} N_{SS}, cm^{-3}$
5×10^{-17}	0.70	0.40	1	2×10^{-16}

Fig. 2 represents the deposition of the different scattering mechanisms (dashed lines describe the appropriate dependence) in total mobility.

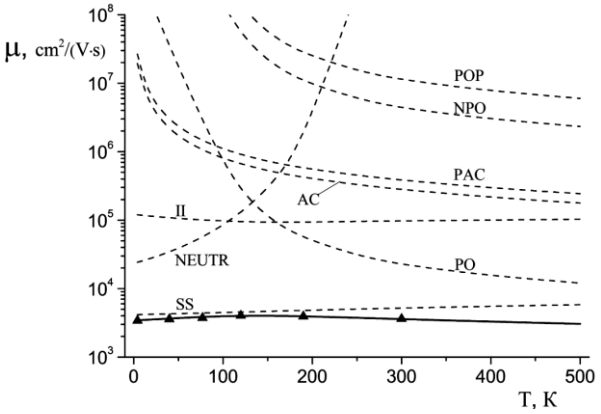

Fig. 2 – The deposition of different scattering modes into total mobility in n-GaSb with donor concentrations $N_D = 5 \times 10^{17}$ cm^{-3}. Solid line – mixed scattering mechanism

One can see that in all temperature range the main scattering mechanism are the static strain scattering. Electron scattering on neutral impurity at low temperatures ($T < 140$ K), on polar optical phonon at higher temperatures and on ionized impurity at all temperature range play also significant role. Other scattering mechanisms – acoustic and piezoacoustic phonon scattering, nonpolar and piezooptic phonon scattering – give negligibly small contributions.

The comparison of the experimental electron mobility data with calculated shown in Table 4.

Table 4 – The comparison of the experimental and calculated electron mobility in n-GaSb wiskers

T, K	μ_{exp}, cm²/(V·s)	μ_{exp}, cm²/(V·s)
4.2	3409	3453
77	3750	3648
120	4020	3970
300	3620	3582

A good coordination between theory and experimental data in the investigated temperature interval is obtained.

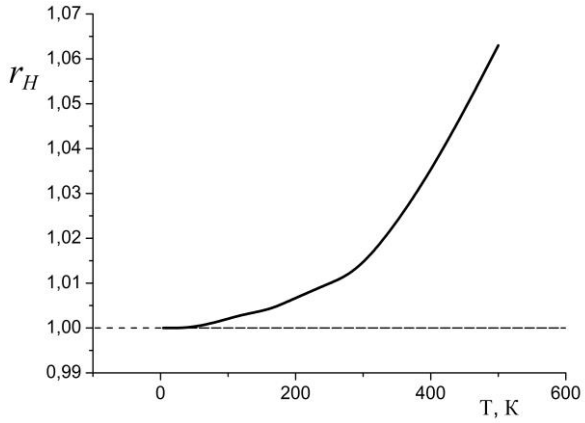

Fig. 3 – The temperature dependence of electron Hall factor in *n*-GaSb

Using the obtained scattering parameters the temperature dependence of electron Hall factor was calculated (see Fig. 3).

The dependece of Hall factors remains close to 1 in all temperature range, which indicates in weak dependence of the calculated parameters on magnetic field.

4. CONCLUSION

The electron scattering effects on the different types of crystal defects in n-GaSb whiskers are considered using the short-range principle. It was shown that in all temperature range the main scattering mechanism is the static strain scattering. Electron scattering on neutral impurity at low temperatures and polar optical phonon at higher temperatures and on ionized impurity at all temperature range play also significant role. Other scattering mechanisms – acoustic and piezoacoustic phonon scattering, nonpolar and piezooptic phonon scattering give negligibly small contributions.

The calculated mobility good coincides with experimental data for GaSb whiskers measured in the temperate interval 4.2-300 K, which indicates in satisfactory description of the crystals by short-range scattering models.

REFERENCES

1. S.H. Hu, C.H. Sun, Y. Sun, J. Ge, R. Wang, N. Dai, *J. Cryst. Growth* **311**, 2309 (2009).
2. M. Yin, G.R. Nash, S.D. Coomber, *Appl. Phys.Lett.* **93**, 121106 (2008).
3. J.B. Rodriguez, L. Cerutti, E. Tournie, *Appl. Phys. Lett.* **94**, 023506 (2009).
4. B.R. Bennett, M.G. Ancona, J.B. Boos, *J. Cryst. Growth* **311**, 47 (2008).
5. O.P. Malyk, *Mater. Sci. Eng. B* **129**, 161 (2006).
6. O.P. Malyk, *phys. status solidi c* **6**, S86 (2009).
7. D.R. Lide, *CRC Handbook of Chemistry and Physics, 82th Edition* (2001).
8. M.E. Straumanis, C.D. Kim, *Acta Crystallogr.* **19**, 256 (1965).
9. M.C. Wu, C.C. Chen, *J. Appl. Phys.* **72**, 4275 (1992).
10. M.W. Heller, R.G. Hamerly, *J. Appl. Phys.* **57**, 4626 (1985).
11. C. Hermann, C. Weisbuch, *Phys. Rev. B* **15**, 823 (1977).
12. A.Ya. Vul', G.I. Bir, Yu.V. Shmartsev, *Sov. Phys. Semicond.* **4** No 12, 2005 (1970).
13. C. Alibert, A. Joullie, A.M. Joullie, C. Ance, *Phys. Rev. B* **27**, 4946 (1983).
14. M.E. Straumanis, C.D. Kim, *J. Appl. Phys.* **36**, 3822 (1965).
15. D.E. Aspnes, A.A. Studna, *Phys. Rev. B* **27**, 985 (1983).
16. V.V. Brazhkin, A.G. Lyapin, V.A. Goncharova, O.V. Stal'gorova, S.V. Popova, *Phys. Rev. B* **56**, 990 (1997).
17. J.D. Wiley, *Semiconductors and Semimetals* (Ed. by R.K. Willardson, A.C. Beer) (Academic Press: N.Y.: **10**, 1975).
18. H.S. Bennett, H. Hung, A. Heckert, *J. Appl. Phys.* **98**, 103705 (2005).
19. P. Giannozzi, S. de Gironcoli, P. Pavone, S. Baroni, *Phys. Rev. B* **43**, 7231 (1991).
20. G. Arlt, P. Quadflieg, *phys. status solidi* **25**, 323 (1968).
21. A.A. Druzhinin, I.P. Ostrovskii, *phys. status solidi c* **1** No 2, 333 (2004).
22. A.A. Druzhinin, I.P. Ostrovskii, Y.N. Khoverko, N.S. Liakh-Kaguy, A.M. Vuytsyk, *Functional Mater.* **21** No 2, 130 (2014).
23. A. Druzhinin, I. Ostrovskii, Y. Khoverko, R. Koretskii, *Mater. Sci. Semiconduct. Proc.* **40**, 766 (2015).
24. O.P. Malyk, *WSEAS Trans. Math.* **3**, 354 (2004).